Journal of Solid State Chemistry 183 (2010) 2445–2450

Contents lists available at ScienceDirect

Journal of Solid State Chemistry

journal homepage: www.elsevier.com/locate/jssc

Annealing effects on the structure, photoluminescence, and magnetic properties of GaN/Mn_3O_4 core–shell nanowires

Hyo Sung Kim [a], Han Gil Na [a], Ju Chan Yang [a], Jong Hoon Jung [b], Yong Sung Koo [b], Nam Jung Hur [b], Hyoun Woo Kim [a,*]

[a] Division of Materials Science and Engineering, Inha University, Incheon 402-751, Republic of Korea
[b] Department of Physics, Inha University, Incheon 402-751, Republic of Korea

ARTICLE INFO

Article history:
Received 15 June 2010
Received in revised form
5 August 2010
Accepted 6 August 2010
Available online 14 August 2010

Keywords:
GaN
Nanowires
Mn_3O_4
Photoluminescence
Thermal annealing

ABSTRACT

Nanowires consisting of GaN/Mn_3O_4 were prepared using a two-step approach that involved dipping the as-synthesized GaN nanowires into an aqueous manganese acetate solution. To examine the effects of annealing, GaN/Mn_3O_4 core–shell nanowires were heated thermally to 700 °C in N_2 ambient. Transmission electron microscopy showed that the continuous Mn_3O_4 shell layer had agglomerated to expose a bare GaN core surface after thermal annealing. The magnetic measurements showed that the ferromagnetic behavior of the GaN nanowires had been suppressed by coating with the Mn_3O_4 shell, without significant change by the subsequent thermal annealing. The GaN/Mn_3O_4 core–shell nanowires exhibited blue, green, and red photoluminescence (PL) emission. The red emission was enhanced by thermal annealing. This paper discusses the associated mechanism for the variations in PL and magnetic properties of GaN/Mn_3O_4 core–shell nanowires.

1. Introduction

Nanocomposites consisting of two or more dissimilar nanoscale structures have attracted increasing attention [1,2]. Among them, composite nanowires are one of the most exciting subjects owing to their specific physical and chemical properties and potential applications in a range of nanoscale devices and systems.

Owing to its useful properties, including a large direct bandgap, strong interatomic bonds and high thermal conductivity [3], gallium nitride (GaN) can be used in blue and ultraviolet light-emitting diodes and laser diodes as well as in high-temperature and high-power optoelectronic devices [4,5]. Therefore, the synthesis of GaN nanowires has been a major research focus [6–8]. Hausmannite (Mn_3O_4) has a normal spinel structure with Mn^{2+} and Mn^{3+} cations in the tetrahedral and octahedral sites, respectively [9]. The extraordinary properties of Mn_3O_4 suggests its potential applications in supercapacitors [10], acetone sensors [11], high-capacity cathode materials for alkaline secondary batteries [12], catalysts for the oxidation of methane [13], and carbon monoxide [14], and a catalyst for the selective reduction of nitrobenzene [15].

In this study, GaN/Mn_3O_4 core–shell nanowires were fabricated by immersing the GaN nanowires into an aqueous manganese acetate solution. With nanophase materials featuring high specific surfaces and reactivity, this composite structure was expected to have useful and interesting properties with potential applications in a range of fields. For example, in lithium ion battery applications, the doped GaN core nanowire functions as an electron transport pathway and stable mechanical support, whereas the Mn_3O_4 shell acts as a structural buffer with good mechanical strength and high capacity. In addition, Mn doping of GaN and/or the presence of Mn_3O_4 are expected to exhibit ferromagnetic behavior below the Curie temperature [16–18]. A Mn_3O_4 shell surrounding the nanowires will have a sufficient surface-to-volume ratio for enhanced gas-sensing and catalytic properties. Furthermore, in optoelectronic applications, it is possible that the photoluminescence (PL) stability of the core nanowires can be enhanced by a shell coating [19] and emission could be generated from the structural defects originating from the heterostructure interface [20]. Composite nanostructures with different materials with excellent physical/chemical properties will also provide a range of novel functionalities.

For potential applications to ultra-large-scale-integration (ULSI) fabrication, the development of a low-temperature process is essential in order to minimize the unintentional diffusion and chemical reactions. Hence, the room-temperature fabrication technique reported in this paper will play an important role in future applications and production. In this study, the structure, morphology, PL and magnetic properties of as-synthesized GaN/Mn_3O_4 core–shell structures were characterized. The effects of thermal heating were also examined because the ULSI fabrication

* Corresponding author. Fax: +82 32 862 5546.
E-mail address: hwkim@inha.ac.kr (H.W. Kim).

0022-4596/$ - see front matter © 2010 Elsevier Inc. All rights reserved.
doi:10.1016/j.jssc.2010.08.006

scheme inevitably involves a thermal heating process. To our knowledge, this is first report of the Mn_3O_4-shelled composite nanowires synthesized using a solution-based approach.

2. Experimental

GaN nanowires were fabricated on gold (Au: about 3 nm)-coated Si substrates by evaporating GaN powder. An alumina boat holding both the substrate and GaN powders was placed inside a quartz tube in a horizontal tube furnace. The distance between the substrate and GaN powder was approximately 10 mm. The Ar and NH_3 flow rates were 100 and 20 sccm, respectively. The reaction temperature was 1000 °C and growth was carried out for 1 h.

To coat the GaN nanowires, 0.4 g of manganese acetate ($Mn(CH_3COO)_2 \cdot 4\,H_2O$) were mixed slowly with 10 mL of deionized (DI) water. All mixtures were stirred vigorously for 10 min. The GaN nanowires-grown substrates were then immersed in the solution for 5 h. The substrates were then annealed at 700 °C for 5 h, in N_2 ambient with a constant flow rate of 1 standard liter per min (slm).

The structure and morphology of the samples were examined by glancing-angle X-ray powder diffraction (XRD, Philips X'pert MRD) with an incidence angle of 0.5°, scanning electron microscopy (SEM, Hitachi S-4200), and transmission electron microscopy (TEM, Philips CM-200) equipped with energy-dispersive X-ray spectroscopy (EDX). The PL measurements were carried out using a He–Cd laser with excitation at 325 nm at 298 K. The magnetic properties of the samples were analyzed using the vibrating sample magnetometer (VMS) option in a physical property measurement system (PPMS), at room temperature (300 K).

3. Results and discussion

Fig. 1a shows the XRD pattern of the solution-treated GaN nanowires prior to thermal annealing. Apart from the diffraction peaks of the hexagonal wurtzite GaN phase (JCPDS card: no. 50-0792), the pattern revealed some weak peaks for an orthorhombic Mn_3O_4 phase with a lattice constant of $a=3.026$, $b=9.769$ Å, and $c=9.568$ Å, (JCPDS card: no. 75-0765). Fig. 1b shows the XRD pattern of the solution-immersed GaN nanowires after thermal annealing at 700 °C. Being similar to Fig. 1a, the entire spectrum was indexed to either the hexagonal wurtzite GaN phase or orthorhombic Mn_3O_4 phase.

Figs. 2a and b show a SEM image and low-magnification TEM image of a solution-treated GaN nanowire, showing a relatively rough surface. The TEM image indicates that the diameter of nanowire ranges from 40 to 80 nm. Fig. 2c exhibits an associated selected area electron diffraction (SAED) pattern, in which the ring spots corresponding to the (020), (002), (022), (100), and (110) lattice planes of orthorhombic Mn_3O_4 structure can be seen. The existence of a ring pattern suggests that the Mn_3O_4 structure is poly-crystalline. Fig. 2d shows an associated lattice-resolved TEM image. A d spacing of 0.28 and 0.30 nm were measured, corresponding to the (110) and (100) planes of orthorhombic Mn_3O_4 (JCPDS card: no. 75-0765). The surface of the Mn_3O_4 structure consisted of several grains, confirming its poly-crystalline nature. TEM suggested that the GaN nanowires were coated completely with a Mn_3O_4 shell layer. Moreover, EDX showed that the composite nanowires were indeed GaN/Mn_3O_4 core–shell nanostructures (see Supplementary materials S-1).

Fig. 3a shows a TEM image of 700 °C-annealed composite nanowires and Fig. 3b shows the associated SAED pattern. The pattern exhibits not only a spot pattern of a hexagonal GaN phase (JCPDS card: no. 50-0792), but also diffraction rings for the

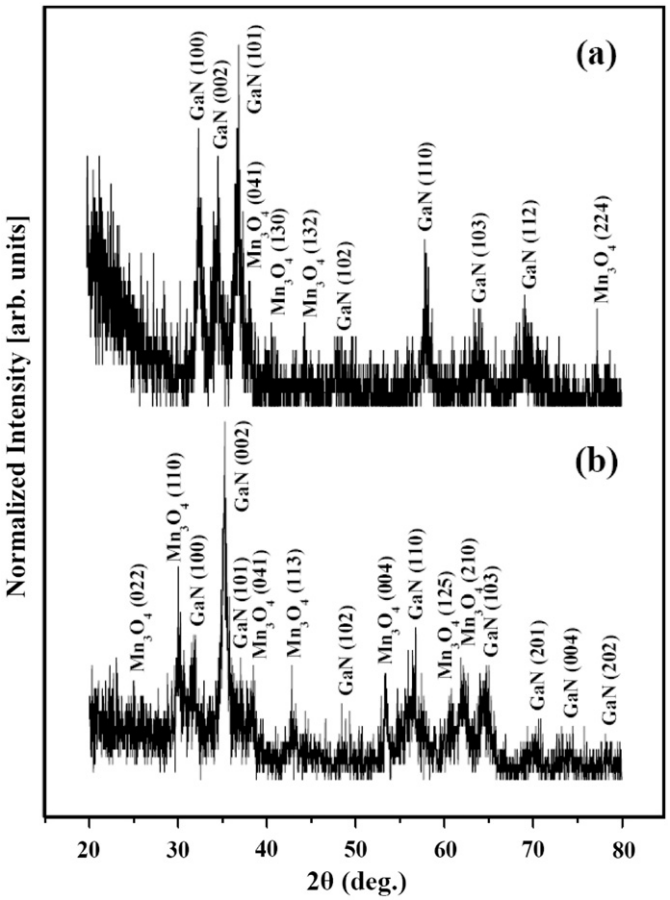

Fig. 1. XRD patterns of the solution-treated GaN nanowires (a) before and (b) after thermal annealing at 700 °C.

orthorhombic Mn_3O_4 phases (JCPDS card: no. 75-0765). The spotty pattern of GaN reveals its single crystal nature, whereas the Mn_3O_4 ring spots correspond to a polycrystalline structure. The corresponding schematic diagrams of the GaN spotty pattern and Mn_3O_4 ring pattern, respectively, are shown in the Suppplementary materials (S-2). Fig. 3c shows a lattice-resolved TEM image taken from the outer region of a nanowire, suggesting that the nanowire consists of hexagonal GaN and orthorhombic Mn_3O_4 phases. The measured lattice spacing of the crystalline plane was 0.27 nm, which corresponds to the (100) and (010) planes of hexagonal GaN. The lattice spacing in the Mn_3O_4 lattice image was 0.26 nm, which corresponds to the (023) plane of orthorhombic Mn_3O_4. Further TEM investigations of the outer surface of the annealed nanowires indicated that some part of the outmost surface contained the hexagonal GaN phase only (Fig. 3d). Although SEM revealed no apparent change in morphology after thermal annealing (see Supplementary materials S-3), TEM suggested that the some of the GaN core nanowires had been exposed presumably by the agglomeration of Mn_3O_4 structures, whereas other parts remained coated with the Mn_3O_4 shell layer.

Fig. 4 shows the magnetic hysteresis curves, measured at 300 K. The curves were corrected for the diamagnetic component arising from the substrate. The right-hand-side graphs show magnified sections of the curve around the zero magnetic field ($H=0$). Parameters, such as the coercive field (H_c), remanent magnetization (M_r), and saturation magnetization (M_S), were compared to evaluate the ferromagnetic behavior.

The H_c, M_r, and M_s for pure GaN nanowires were approximately 0.132 kOe, 4×10^{-6} emu, and 2.2×10^{-5} emu, respectively, whereas

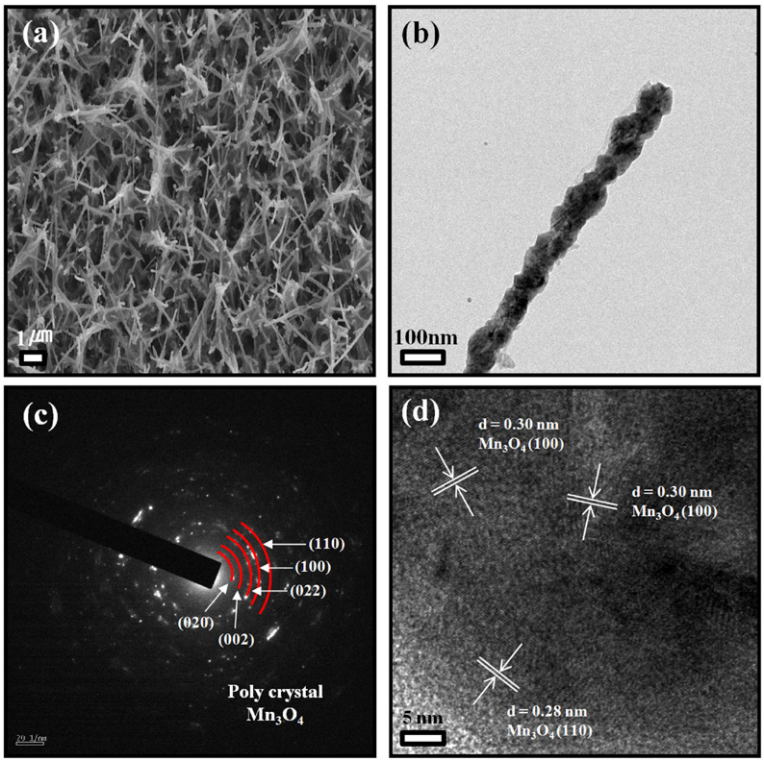

Fig. 2. (a) SEM image, (b) low-magnification TEM image, (c) SAED pattern, and (d) lattice-resolved TEM image of a solution-treated GaN nanowire.

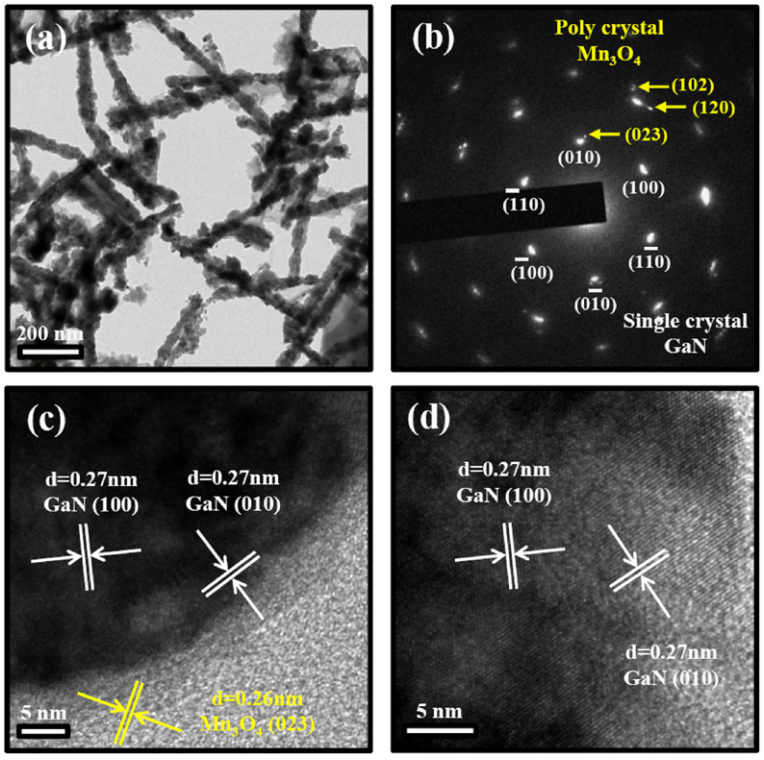

Fig. 3. (a) Low-magnification TEM image of 700 °C-annealed core–shell nanowires. (b) Corresponding SAED pattern. (c,d) Lattice-resolved TEM image enlarging an area near the surface of the nanowire.

they were approximately 0.118 kOe, 2×10^{-6} emu, and 0.9×10^{-5} emu, respectively, for the Mn_3O_4/GaN composite nanowires (Figs. 4a and b). The pure GaN nanowires exhibited weak ferromagnetism. The room-temperature ferromagnetism was previously reported in undoped GaN nanoparticles [21]. The ferromagnetism of undoped GaN mainly originates from Ga vacancies [22,23].

The ferromagnetic behavior of the core–shell nanowires was depressed slightly compared to that of the pure GaN nanowires.

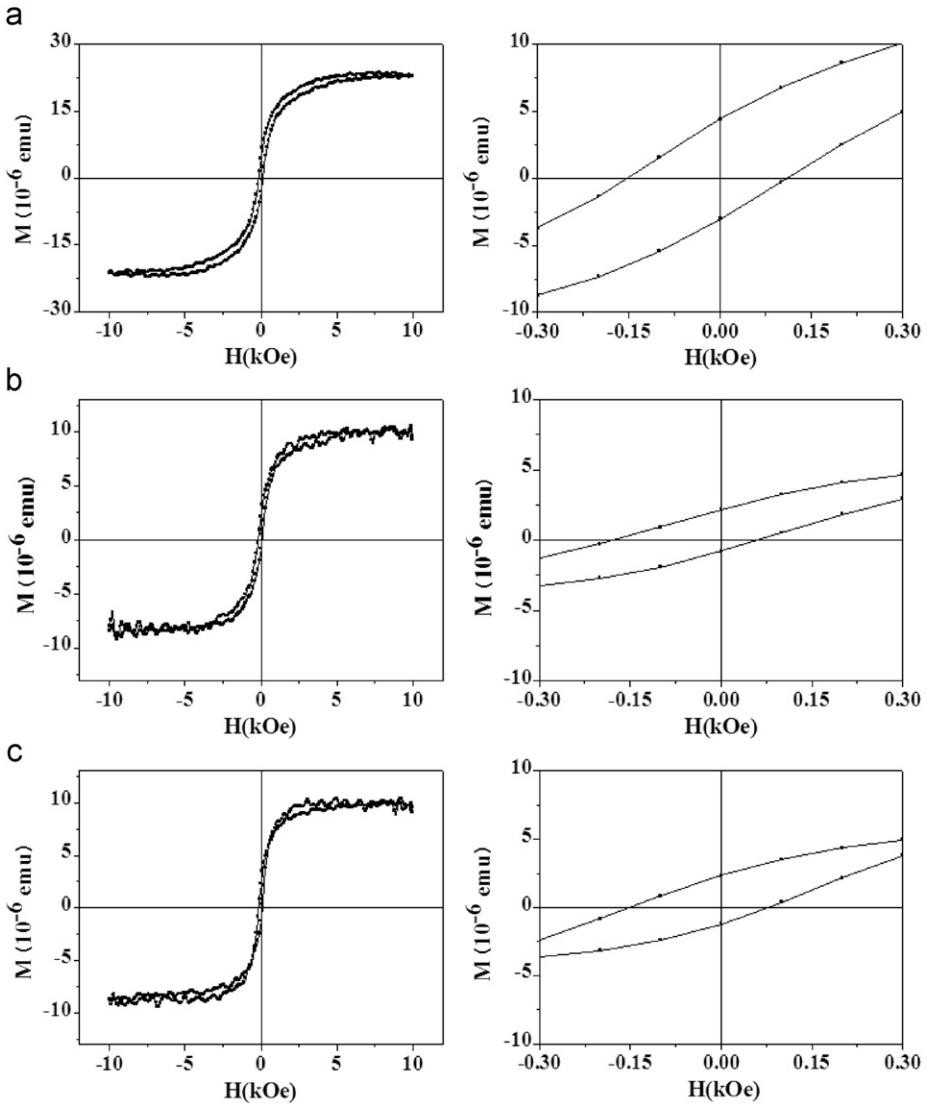

Fig. 4. *M–H* curve measured at 300 K for (a) core GaN nanowires, (b) GaN/Mn_3O_4 core–shell nanowires, and (c) annealed core–shell nanowires (M_s: saturated magnetization; *M*: magnetization; *H*: magnetic field). The right-hand-side curves show the magnified section of the curve around a zero magnetic field.

Mn_3O_4 only shows ferromagnetic ordering below its Curie temperature (T_C; ~38–51 K), regardless of its morphology [16–18,24–27]. Accordingly, the Mn_3O_4 structure should exhibit paramagnetic behavior at 300 K rather than ferromagnetic behavior and thus the addition of a paramagnetic Mn_3O_4 structure to the GaN core nanowires cannot affect the ferromagnetic ability. It is possible that Mn doping affects the ferromagnetic behavior. However, XRD and TEM did not confirm the existence of ferromagnetic second phases, such as Mn_4N [28], Mn_3GaN [29], and Mn_3Ga [30]. The XRD pattern of the pure GaN nanowires, as-synthesized and annealed composite nanowires were compared to identify the GaMnN (i.e. solid solution (Ga,Mn)N structure) phase (see Supplementary materials S-4). Since the atomic of Mn is smaller than that of Ga, it is expected that the substitutional incorporation of Mn would reduce the lattice constants of the GaN lattice. However, there was no evidence of a shift in the main GaN peaks to more positive values by the shell coating (see Supplementary materials S-4 (a,b)). Accordingly, it is possible that crystallinity of GaN structure has been degraded by the Mn_3O_4 coating. It is evident that the full width at half maximum (FWHM) values of major GaN peak were increased by the coating (see Supplementary materials S-4 (a,b)) and the peak-broadening is originated from the disorder induced by the coating. Although it is not clear at this moment, it is surmised that the disorder or defects induced in the GaN/Mn_3O_4 interface could have degraded the crystallinity. On the other hand, H_c, M_r, and M_s of the composite nanowires were nearly invariant by the thermal heat treatment. The H_c, M_r and M_s for annealed Mn_3O_4/GaN composite nanowires were approximately 0.114 kOe, 2×10^{-6} and 0.9×10^{-5} emu, respectively (Fig. 4c). XRD confirmed that no new phase was generated by thermal annealing. In addition, the unit volume of the GaN hexagonal structure was estimated by measuring the positions of the major GaN XRD peaks related to the *a* and *c* lattice constants (see Supplementary materials S-4 and SI-5). There was no evidence of a decrease in the unit volume of GaN by thermal annealing, which means that no substitutional diffusion of Mn into GaN lattice had occurred by the thermal annealing. Furthermore, it is unlikely that the thermal annealing noticeably enhanced the crystallinity of GaN phase. Although the above observations supported the invariance of ferromagnetic behavior by the thermal annealing at 700 °C, further detailed investigation is underway.

PL measurements were carried out on the core GaN nanowires, as-fabricated GaN/Mn_3O_4 core–shell nanowires and Mn_3O_4-coated

nanowires annealed at 700 °C. The PL intensity was decreased significantly by the Mn_3O_4 coating (see Supplementary materials S-6). However, the overall PL intensity of the core–shell nanowires was relatively unaffected by subsequent thermal annealing. Fig. 5a shows the PL spectrum of the as-synthesized GaN/Mn_3O_4 core–shell nanowires, measured at room temperature. This emission can be deconvoluted into three peaks, centered at 2.9, 2.4, and 1.7 eV corresponding to the blue, green and red regions, respectively. The green and blue emissions are associated with vacancy-related structural defects, including V_{Ga}, $V_{Ga}-O_N$ complexes [31–34]. On the other hand, the red emission band in GaN was assigned to the vacancy–impurity pairs, including V_{Ga}Si, V_NMg, V_NC_N, and $V_{Ga}O_N$ [35–39]. For example, a red emission process through a donor–acceptor pair (DAP) transition process involving a deep donor V_NC_N and deep acceptor $V_{Ga}O_N$ was suggested [38,39]. Since the dopant was not intentionally introduced in this synthesis route, the origin of red emission can be attributed to the impurities, such as C and O, which might have originated from inside the chamber during the synthetic process. Fig. 5b shows the PL spectrum of the GaN/Mn_3O_4 core–shell nanowires annealed at 700 °C. A comparison of Figs. 5b and a shows that the intensity of red emission was reduced significantly by thermal annealing. These results suggest tentatively that annealing in N_2 ambient reduces the number of nitrogen vacancies (V_N). Accordingly, the number of vacancy–impurity pairs, including V_NMg and V_NC_N would be reduced, ultimately quenching the red light emission from the GaN lattice. However, further study to reveal the detailed mechanism of the intensity variations is currently underway.

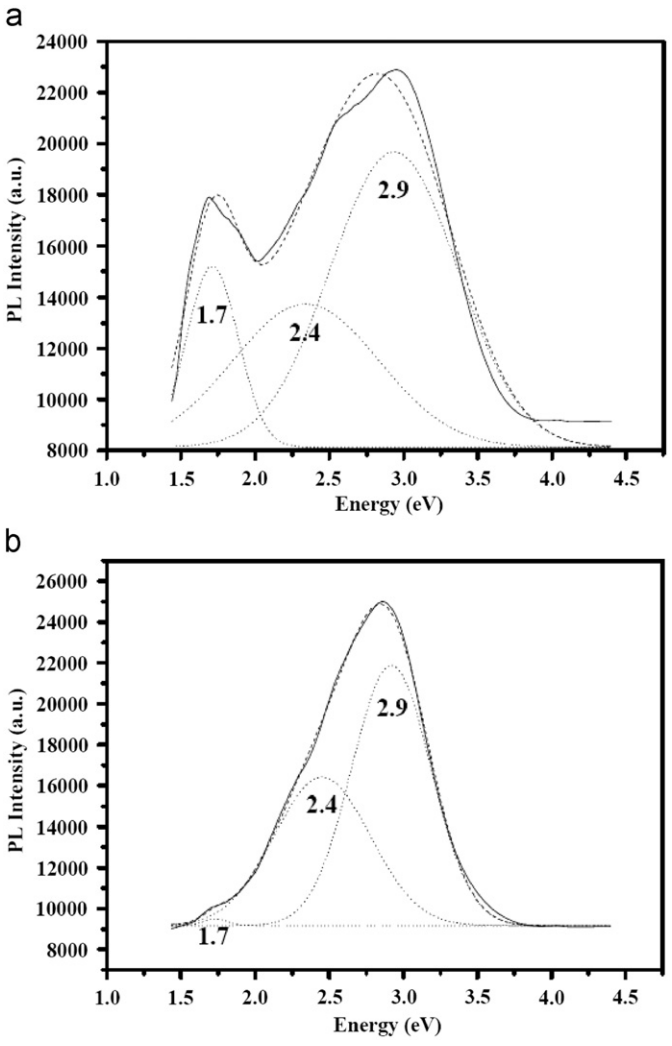

Fig. 5. Integrated PL intensities of GaN/Mn_3O_4 core–shell nanowires: (a) before and (b) after thermal annealing.

4. Conclusions

GaN core/Mn_3O_4-shell nanowires were fabricated and the effects of a subsequent thermal annealing process were investigated. SEM indicated that no significant morphological change had occurred after thermal annealing. XRD showed that the core–shell nanowires were comprised of hexagonal GaN and orthorhombic Mn_3O_4 phases, regardless of subsequent thermal annealing at 700 °C. With the GaN core being fully coated with a Mn_3O_4 shell, some parts of the GaN core had been exposed by the agglomeration of Mn_3O_4 caused by thermal annealing. The pure GaN nanowires exhibited weak ferromagnetism at 300 K. The ferromagnetic behavior was evaluated with respect to a coercive field, remanent magnetization and saturation magnetization in the hysteresis loop. Although the decrease in ferromagnetic behavior by the solution coating was attributed to the degradation of crystallinity of GaN structure, the thermal annealing did not affect the ferromagnetic behavior. The PL spectra of the GaN/Mn_3O_4 core–shell nanowires were deconvoluted into three broad bands centered at 2.9, 2.4, and 1.7 eV. The integrated intensity of red emission from the core–shell nanowires was decreased significantly by annealing in N_2 ambient, presumably due to the elimination of nitrogen vacancies.

Acknowledgments

This research was supported by National Nuclear R&D Program through the National Research Foundation of Korea (NRF) funded by the Ministry of Education, Science and Technology (2010-0018699).

Appendix A. Supporting information

Supplementary data associated with this article can be found in the online version at doi:10.1016/j.jssc.2010.08.006.

References

[1] P.M. Ajayan, L.S. Schadler, P.V. Braun, in: Nanocomposite Science and Technololgy, Wiley-VCH Verlag, Weinheim, Germany, 2003.
[2] T.T. Xu, F.T. Fisher, L.C. Brinson, R.S. Ruoff, Nano Lett. 3 (2003) 1135.
[3] J. Neugebauer, C.G. Van de Walle, Appl. Phys. Lett. 69 (1996) 503.
[4] B. Liu, Y. Bando, C. Tang, F. Xu, J. Hu, D. Golberg, J. Phys. Chem. B 109 (2005) 17082.
[5] H.Q. Jia, L.W. Guo, W.X. Wang, H. Chen, Adv. Mater. 45 (2009) 4641.
[6] Y. Huang, X. Duan, Y. Cui, C.M. Lieber, Nano Lett. 2 (2002) 101.
[7] H.M. Kim, Y.H. Choo, H. Lee, S.I. Kim, S.R. Ryu, D.Y. Kim, T.W. Kang, K.S. Chung, Nano Lett. 4 (2004) 1059.
[8] J. Chen, C. Xue, H. Zhuang, Z. Yang, L. Qin, H. Li, Y. Huang, J. Alloys Compd. 468 (2009) L1.
[9] S. Fritsch, J. Sarrias, A. Rousset, G.U. Kulkarni, Mater. Res. Bull. 33 (1998) 1185.
[10] D.P. Dubal, D.S. Dhawale, R.R. Salunkhe, S.M. Pawar, V.J. Fulari, C.D. Lokhande, J. Alloys Compd. 484 (2009) 218.
[11] L. Zhang, Q. Zhou, Z. Liu, X. Hou, Y. Li, Y. Lv, Chem. Mater. 21 (2009) 5066.
[12] J. Pan, Y. Sun, Z. Wang, P. Wan, M. Fan, J. Alloys Compd. 470 (2009) 75.
[13] G.D. Moggridge, T. Rayment, R.M. Lambert, J. Catal. 134 (1992) 242.
[14] E.R. Stobhe, B.A.D. Boer, J.W. Deus, Catal. Today 47 (1999) 161.
[15] W.M. Wang, Y.N. Yang, J.Y. Zhang, Appl. Catal. A 133 (1995) 81.
[16] G. Srinivasan, M.S. Seehra, Phys. Rev. B 28 (1983) 1.
[17] K. Dwight, N. Menyuk, Phys. Rev. 119 (1960) 1470.
[18] D.P. Norton, S.J. Pearton, A.F. Hebard, N. Theodoropoulou, L.A. Boatner, R.G. Wilson, Appl. Phys. Lett. 82 (2003) 239.
[19] C.-C. Wang, C.-C. Kei, Y. Tao, Y.-P. Perng, Electrochem. Solid State Lett. 12 (2009) K49.
[20] M. Lei, L.Q. Qian, Q.R. Hu, S.L. Wang, W.H. Tang, J. Alloys Compd. 487 (2009) 568.

[21] C. Madhu, A. Sundaresan, C.N.R. Rao, Phys. Rev. B 77 (2008) 201306 R.
[22] H. Jin, Y. Dai, B.B. Huang, M.-H. Whangbo, Appl. Phys. Lett. 94 (2009) 162505.
[23] P. Dev, Y. Xue, P. Zhang, Phys. Rev. Lett. 100 (2008) 117204.
[24] Y.Q. Chang, X.Y. Xu, X.H. Luo, C.P. Chen, D.P. Yu, J. Cryst. Growth 264 (2004) 232.
[25] T. Ozkaya, A. Baykal, H. Kavas, Y. Köseoglu, M.S. Toprak, Physica B 403 (2008) 3760.
[26] L.-X. Yang, Y.-J. Zhu, H. Tong, W.-W. Wang, C.-F. Cheng, J. Solid State Chem. 179 (2006) 1225.
[27] Y.Q. Chang, D.P. Yu, Y. Long, J. Xu, X.H. Luo, R.C. Ye, J. Cryst. Growth 279 (2005) 88.
[28] R. Frazier, G. Thaler, M. Overberg, B. Gila, C.R. Abernathy, S.J. Pearton, Appl. Phys. Lett. 83 (2003) 1758.
[29] I.T. Yoon, T.W. Kang, D.J. Kim, Mater. Sci. Eng. B 134 (2006) 49.
[30] N. Theodoropoulou, K.P. Lee, M.E. Overberg, S.N.G. Chu, A.F. Hebard, C.R. Abernathy, S.J. Pearton, R.G. Wilson, J. Nanosci. Nanotechnol. 1 (2001) 101.
[31] M.A. Reshchikov, H. Morkoc, S.S. Park, K.Y. Lee, Appl. Phys. Lett. 78 (2001) 3041.
[32] M.A. Reshchikov, H. Morkoc, J. Appl. Phys. 97 (2005) 061301.
[33] M.A. Reshchikov, R.Y. Korotkov, Phys. Rev. B 64 (2001) 115205.
[34] H.C. Yang, T.Y. Lin, Y.F. Chen, Phys. Rev. B 62 (2000) 12593.
[35] S. Nakamura, N. Iwasa, M. Senoh, T. Mukai, Jpn. J. Appl. Phys. 31 (1992) 1258.
[36] U. Kaufmann, M. Kunzer, H. Obloh, M. Maier, Ch. Manz, A. Ramakrishnan, B. Santic, Phys. Rev. B 59 (1999) 5561.
[37] D.M. Hofmann, B.K. Meyer, H. Alves, F. Leiter, W. Burkhard, N. Romanov, Y. Kim, J. Krüger, E.R. Weber, Phys. Status Solidi A 180 (2000) 261.
[38] L. Wang, E. Richter, M. Weyers, Phys. Status Solidi A 204 (2007) 846.
[39] S. Zeng, G.N. Aliev, D. Wolverson, J.J. Davies, S.J. Bingham, D.A. Abdulmalik, P.G. Coleman, T. Wang, P.J. Parbrook, Phys. Status Solidi C 3 (2006) 1919.